MOLECULAR AND CELLULAR BIOLOGY, Mar. 2007, p. 2215–2228 Vol. 27, No. 6
0270-7306/07/$08.00+0 doi:10.1128/MCB.01454-06

Colitis and Colitis-Associated Cancer Are Exacerbated in Mice Deficient for Tumor Protein 53-Induced Nuclear Protein 1▽

Julien Gommeaux,[1,2]† Carla Cano,[1,2]† Stéphane Garcia,[1,2] Meritxell Gironella,[1,2] Sylvia Pietri,[3] Marcel Culcasi,[3] Marie-Josèphe Pébusque,[1,2] Bernard Malissen,[4] Nelson Dusetti,[1,2] Juan Iovanna,[1,2] and Alice Carrier[1,2]*

INSERM, U624 Stress cellulaire, F-13288 Marseille, France[1]; Aix-Marseille Université, Campus de Luminy, F-13000 Marseille, France[2]; Aix-Marseille Université, Faculté des Sciences de Saint-Jérôme, SREP-Sondes Moléculaires en Biologie, CNRS UMR6517, F-13397 Marseille, France[3]; and Aix-Marseille Université, Centre d'Immunologie de Marsaille-Luminy, F-13288 Marseille, France[4]

Received 7 August 2006/Returned for modification 7 September 2006/Accepted 19 December 2006

Tumor protein 53-induced nuclear protein 1 (TP53INP1) is an antiproliferative and proapoptotic protein involved in cell stress response. To address its physiological roles in colorectal cancer and colitis, we generated and tested the susceptibility of *Trp53inp1*-deficient mice to the development of colorectal tumors induced by injection of the carcinogen azoxymethane followed by dextran sulfate sodium (DSS)-induced chronic colitis. *Trp53inp1*-deficient mice showed an increased incidence and multiplicity of tumors compared to those of wild-type (WT) mice. Furthermore, acute colitis induced by DSS treatment was more severe in *Trp53inp1*-deficient mice than in WT mice. Treatment with the antioxidant *N*-acetylcysteine prevented colitis and colitis-associated tumorigenesis more efficiently in WT mice than in *Trp53inp1*-deficient mice, suggesting a higher oxidative load in the latter. Consistently, we demonstrated by electron spin resonance and spin trapping that colons derived from deficient mice produced more free radicals than those of the WT during colitis and that the basal blood level of the antioxidant ascorbate was decreased in *Trp53inp1*-deficient mice. Collectively, these results indicate that the oxidative load is higher in *Trp53inp1*-deficient mice than in WT mice, generating a more-severe DSS-induced colitis, which favors development of colorectal tumors in *Trp53inp1*-deficient mice. Therefore, TP53INP1 is a potential target for the prevention of colorectal cancer in patients with inflammatory bowel disease.

Colorectal cancer is the second-most-common type of cancer in Western countries, resulting in about 55,000 deaths (10% of cancer deaths) in the United States in 2005. Patients with chronic inflammatory bowel disease, either ulcerative colitis or Crohn's disease, are at increased risk of developing CRC (22, 36), indicating that chronic intestinal inflammation is a major risk for CRC (47, 67). Consistently, anti-inflammatory therapies with nonsteroidal anti-inflammatory drugs such as aspirin reduce the risk of cancer (10, 18). Chronic inflammation is characterized by episodes of active inflammation (flare-ups) separated by periods of disease inactivity (remission). Active inflammation involves activation and recruitment of leukocytes (neutrophils, eosinophils, and monocytes, which differentiate locally into macrophages), and tissue mast cells also have a significant role (11). Leukocytes and phagocytic cells secrete proinflammatory cytokines and chemokines, as well as growth factors and matrix-degrading enzymes, which have a deep impact on the cells of the local microenvironment. Inflammatory cells also release reactive oxygen species and reactive nitrogen species that are normally produced to repel infection. However, uncontrolled inflammation is associated with oxidative stress and oxidative cellular damage. DNA lesions form either directly when ROS modify bases or indirectly as a consequence of lipid peroxidation products that react with DNA (21, 31, 34, 66). In proliferating cells, oxidative DNA lesions induce mutations that are commonly observed in mutated oncogenes and tumor suppressor genes, such as the gene encoding tumor suppressor p53 (20). ROS and RNS promote oncogenesis by altering cell proliferation and cell death (15, 63). Therefore, oxidative stress and oxidative cellular damage, which are hallmarks of IBD, play key roles in the pathogenesis of this disease and in IBD-associated carcinogenesis (21, 52).

TP53INP1, also known as TEAP (7), SIP (60), and p53DINP1 (39), is a newly described factor involved in cell stress response. The gene encoding TP53INP1 is ubiquitously expressed, with higher expression levels in the thymus and other lymphoid organs (7). In vitro, *TP53INP1* expression is up-regulated in different cell types upon treatment with agents inducing cell proliferation arrest and/or apoptosis, including oxidative stress agents (3, 25, 35, 39, 55, 60, 64, 70). *TP53INP1* expression is induced by p53, which exerts its function mainly by inducing transcription of target genes involved in cell cycle arrest and apoptosis, as part of the cell response to genotoxic stress (39, 59). Induction of *TP53INP1* is not always dependent on p53 but can involve p73 or E2F1 transcription factors, which also play roles in cell proliferation and apoptosis (19, 61). The *TP53INP1* gene encodes two protein isoforms, TP53INP1α and TP53INP1β, both of which induce cell cycle arrest and apoptosis when overexpressed (60). The sequences of these

* Corresponding author. Mailing address: INSERM, U624 Stress cellulaire, Case 915 Parc Scientifique de Luminy, 13288 Marseille Cedex 9, France. Phone: 33 4 91 82 75 53. Fax: 33 4 91 82 60 83. E-mail: carrier@marseille.inserm.fr.

† These authors contributed equally to this work.

▽ Published ahead of print on 22 January 2007.

proteins do not contain any known functional domain except for a PEST domain generally found in proteins with a short half-life. TP53INP1 physically interacts with the homeodomain-interacting protein kinase 2, HIPK2, and with the proapoptotic PKCδ upon exposure to genotoxic agents, contributing to regulation of p53 activity during apoptosis (58, 69). In vivo, the *TP53INP1* gene is overexpressed during pancreatic inflammation (14, 24). Conversely, its expression is lost in rat preneoplastic lesions in liver (37, 54) and during gastric cancer progression in humans, which correlates with a decreased level of tumor cell apoptosis and a poor prognosis (23). Altogether, currently available data point to a role of TP53INP1 in cellular homeostasis through its antiproliferative and proapoptotic activities. Therefore, loss of *TP53INP1* expression may contribute to deregulation of cell proliferation and death, which are hallmarks of oncogenesis.

To address the putative role of *TP53INP1* as a tumor suppressor, we generated mice lacking expression of its mouse ortholog, namely *Trp53inp1*. Herein, we show increased susceptibility of *Trp53inp1*-deficient mice to experimental induction of colorectal tumorigenesis and acute colitis. Furthermore, using electron spin resonance techniques, we found a higher level of ROS production both in untreated and colitic *Trp53inp1*-deficient mouse colons than in WT colons. Therefore, a higher level of oxidative stress in *Trp53inp1*-deficient colons may provide a mechanism for increased tissue damage and colorectal carcinogenesis in these mice.

MATERIALS AND METHODS

Abbreviations used. The following abbreviations are used in this report: AFR, ascorbyl free radical; ANOVA, analysis of variance; AOM, azoxymethane; CAT, catalase; CRC, colorectal cancer; DAI, disease activity index; DEPMPO, 5-(diethoxyphosphoryl)-5-methyl-1-pyrroline *N*-oxide; DMEM, Dulbecco's modified Eagle's medium; DMSO, dimethyl sulfoxide; DSS, dextran sulfate sodium; ES, mouse embryonic stem cells; ESR, electron spin resonance; H&E, hematoxylin and eosin; H_2O_2, hydrogen peroxide; $HO^{\cdot}$, hydroxyl radical; IBD, inflammatory bowel disease; NAC, *N*-acetylcysteine; O_2^{-}, superoxide; PBS, phosphate-buffered saline; PKCδ, protein kinase C δ; RNS; reactive nitrogen species; ROS, reactive oxygen species; RT, reverse transcription; SD, standard deviation; SE, standard error; SOD, superoxide dismutase; TBARS, thiobarbituric acid-reactive substances; TP53INP1, tumor protein 53-induced nuclear protein 1; WT, wild type.

Gene targeting and generation of *Trp53inp1*-deficient mice. The *Trp53inp1* gene was targeted by homologous recombination in ES cells, as described elsewhere (68), except that the neomycin selection cassette contained the gene encoding Cre recombinase, designed for self-excision in the male germ line (6). Briefly, the linearized targeting vector was electroporated into 129/Sv ES cells, and G418/Geneticin-resistant clones were screened by Southern blotting for correct integration of the cassette, using probes flanking the deleted region as well as a *Neo*-derived probe to verify the number of insertions of the cassette (the protocol and sequences are available upon request). Two recombinant clones were identified and independently injected into BALB/c blastocysts to generate chimeric mice. Chimeric males were mated to C57BL/6 females to generate heterozygous pups without the neomycin selection cassette. Genotype analyses were done on genomic DNA from tail biopsies with PCR primers F (5′-AATG TATGCAATCTTAGCTGATGC-3′), R1 (5′-TCTTGAGGTAACATAGTGA AATGC-3′), and R2 (5′-CCAAACACTGTCACTGTATTGATA-3′). Mice heterozygous for the mutation on a mixed 129/Sv by C57BL/6 background were intercrossed to generate homozygous mutants (*Trp53inp1*$^{-/-}$) and WT littermates (*Trp53inp1*$^{+/+}$). Absence of mRNA expression was confirmed by RT-PCR with primers Ex1F (5′-CGCAGCTACCTCAGCAC-3′), Ex5R (5′-TGTTCCAA AAATGTTGCCTG-3′), and Ex6R (5′-TTTTGGCCACGACATCTGTA-3′) for *Trp53inp1* and RL3-F (5′-GAAAGAAGTCGTGGAGGCTG-3′) and RL3-R (5′-ATCTCATCCTGCCCAAACAC-3′) for *RL-3*. The mice were housed in specific-pathogen-free conditions in accordance with institutional guidelines. All experimental protocols were in accordance with French laws and European directives.

Western blotting. For Western blot analysis, fibroblasts derived from *Trp53inp1*$^{+/+}$ and *Trp53inp1*$^{-/-}$ embryos were treated with 0.1 mM H_2O_2 (Sigma-Aldrich) for 1 h, then allowed to recover in DMEM–10% fetal calf serum for 5 h. The proteins in the lysates were quantified and analyzed by Western blotting, as previously described (58). Incubation was performed using an in-house monoclonal antibody recognizing both isoforms of TP53INP1.

Tumor induction. AOM is a procarcinogen with structural similarities to cycasin, a natural compound that strongly induces tumors in the colons and rectums of humans and animals. AOM causes the formation of O^6-methylguanine adducts in DNA, which can lead to G→A transitions after replication. It induces tumors in the distal colon of rodents and is commonly used in experimental protocols of colorectal cancer for mechanistic exploration or screening of potential drugs (46). DSS is the most widely used toxic chemical agent in experimental models of IBD (52). Repeated administration of DSS enhances the formation of AOM-induced tumors (41, 56) by mimicking chronic ulcerative colitis (40). *Trp53inp1*-deficient mice and their WT littermates (7 to 10 weeks old) were injected intraperitoneally with 12.5 mg/kg AOM (Sigma). After 5 days, 2.5% DSS (molecular weight, 36,000 to 50,000; MP Biomedicals) was given in their drinking water for 5 days, followed by 16 days of tap water. This cycle was repeated twice (5 days of 2.5% DSS and 4 days of 2% DSS), and the mice were sacrificed 10 days after the last cycle. When specified, the mice were also given 10 mg/ml NAC (Sigma) in their drinking water continuously for 8 days before being injected with AOM and continuously during the entire protocol until they were sacrificed. To induce tumors by AOM or DSS alone, the mice were either treated with a single injection of AOM without further DSS treatment or mock-injected with PBS, followed by three cycles of DSS. They were sacrificed either at 9 weeks after injection (corresponding to the timeline of AOM-DSS protocol) or at 7 months after injection to assess the long-term effects of either treatment. In the latter case, for tumor induction by DSS alone, an additional DSS cycle (4 days of 2% DSS) was performed 11 weeks after the injection of PBS.

Induction and analysis of acute colitis. Treatment with DSS leads to acute colonic inflammation with superficial ulceration, mucosal damage, and leukocyte infiltration. DSS is toxic to mucosal epithelial cells, and the eventual dysfunction of the mucosal barrier leads to mucosal inflammation (30). Mice (7 to 10 weeks old) were given 3.5% DSS in drinking water for 7 days, after which they were given water only until they were sacrificed. Every day during and after the administration of DSS, the mice were monitored for weight loss, pathological features (rectal bleeding and diarrhea), and survival. When specified, the mice were also given 10 mg/ml of NAC in their drinking water continuously for 10 days before, during, and after the administration of DSS until they were sacrificed. The animals were weighed, and the value was expressed as a percentage of the initial weight on day 0 of the protocol. They were also inspected for visible clinical signs of pathology. The presence of diarrhea, rectal bleeding, and weight loss were separately graded on a 0 to 3 scale (Table 1), and the average of the three values constitutes the DAI. Additionally, colitic mice were sacrificed at various time points, and their colons were removed for histological analysis.

Morphological and immunohistochemical analyses. The colons were removed, cut open longitudinally, rinsed free of feces with PBS, and fixed flat in 4% formaldehyde at 4°C overnight. The following day, the colons were carefully dried on blotting paper, weighed, measured, and photographed at high resolution. For each individual colon, the weight-to-length ratio was determined, in milligrams per millimeter of colon. The colon samples were then embedded in paraffin as "Swiss rolls" containing the full-length organ. Sections 5 μm thick were stained with H&E for histopathological assessment of colitis and tumors. Crypt damage was scored as previously described (65): 0, no damage; 1, basal 1/3 damaged; 2, basal 2/3 damaged; 3, only surface epithelium intact; or 4, entire crypt and epithelium lost. The score of each parameter was multiplied by a factor reflecting the percentage of tissue involvement (×1, 0 to 25%; ×2, 26 to 50%; ×3, 51 to 75%; ×4, 76 to 100%). PCNA immunostaining was performed using PC10 clone antibody and animal research kits (Dako, Carpinteria, CA) according to the manufacturer's instructions. Apoptosis was studied using an anti-active caspase-3 antibody (Promega, Madison, WI) on a Ventana benchmark device with Ventana kits (Ventana, Tucson, AZ). Staining of the tumor surface, PCNA, and active caspase-3 was assessed by image analysis on a Samba 2050 device (Samba Technology, Meylan, France). Each slide was digitalized, and the edges of the tumors were manually delimited and then analyzed. Tumor proliferation and apoptosis indices (for PCNA and active caspase-3 staining, respectively) were expressed as percentages of the tumoral surface.

Immunohistofluorescence. Colon cryosections (10 μm) were air-dried, fixed in acetone for 5 min, and washed in PBS before being saturated in blocking buffer (2.5% bovine serum albumin, 5% normal goat serum, 10% anti-FcR hybridoma

TABLE 1. Criteria for scoring the disease activity index[a]

Score	Criterion		
	Weight loss (% of initial wt)	Stool consistency	Rectal bleeding
0	<1	Normally formed pellets	None
1	1–4.99	Soft pellets not adhering to the anus	Small spots of blood in stool; dry anal region
2	5–10	Very soft pellets adhering to the anus	Large spots of blood in stool; blood appears through anal orifice
3	>10	Liquid stool on long streams; wet anus	Deep red stool; blood spreads largely around the anus

[a] Criteria have been modified from the work of Soriano et al. (53).

supernatant) for 30 min. Then the sections were stained in 0.5× blocking buffer with fluorescein isothiocyanate-conjugated rat anti-mouse B220, CD3ε, or Gr1 monoclonal antibody (eBiosciences) or with purified rabbit anti-mouse NF-κB (p65) polyclonal antibody (Santa Cruz) for 1 h at room temperature in a humid chamber. The NF-κB staining was revealed using Alexa Fluor 546-conjugated goat anti-rabbit polyclonal antibody (Invitrogen). The nuclei were stained with Hoechst 33258 (Invitrogen). Photographs were taken at ×40 magnification, and quantification was performed. For quantification of the NF-κB-stained samples, no less than 250 nuclei were counted per slide. For quantification of immune cell infiltration, no less than 25 crypts were counted per animal.

ESR studies and lipid peroxidation assay. The spin trap DEPMPO was synthesized as previously described (16). For determination of the AFR-DMSO content by ESR, blood was drawn from either anesthetized *Trp53inp1*-deficient or WT mice at day 2 of DSS-induced acute colitis or from untreated mice. The blood was collected in heparinized tubes which were immediately inverted five times and stored at room temperature for 2 h. Plasma samples were prepared by centrifugation (4,700 × g; 10 min; 4°C) and immediately frozen in liquid nitrogen. Prior to being analyzed by ESR, the plasma samples were thawed, and 1 volume of DMSO (Sigma-Aldrich) was added. For spin-trapping experiments, the samples were prepared as follows: the colons were removed from untreated or DSS-treated mice at day 2 of colitis, cut into small pieces, and split into three equal parts which were separately cultured either in medium alone (DMEM, 10% fetal bovine serum, 1% penicillin/streptomycin; all from Invitrogen) or in medium containing 100 U/ml SOD (Sigma-Aldrich) or 5,000 U/ml CAT (Sigma-Aldrich). After 1 h, aliquots of aqueous DEPMPO were added to the culture medium to reach final concentrations of 10 mM. After 5-min incubations with the spin trap, the supernatants of the colon cultures were immediately frozen in liquid nitrogen. Thawed samples were quickly introduced into a standard aqueous flat cell which was fitted within the cavity of a Bruker ESP 300 (Karlsruhe, Germany) X-band (9.8 GHz) ESR spectrometer equipped with a TM110 cavity and operating at a field modulation of 100-kHz and a microwave power of 10 mW. Spectral acquisition was initiated at room temperature 60 s after either the addition of DMSO or the complete thawing of the DEPMPO-supplemented samples. Instrument settings for the AFR-DMSO (spin-trapping) experiments were as follows: modulation amplitude, 0.1 mT (0.05 mT); time constant, 163.8 ms (20.5 ms); receiver gain, 4×10^5 (2×10^5); scan rate, 0.05 mT · s^{-1} (0.29 mT · s^{-1}); number of accumulated scans, 2 (1). Assignment of the ESR signals was performed according to the literature (16, 42, 44). Free-radical concentrations were derived from double integrals of the simulated spectra obtained with either WinSim software (13) or the program of Rockenbauer and Korecz (48). Data (arbitrary units) are expressed as means ± SDs, with 3 to 7 independent experiments per group. The lipid peroxidation level in plasma, a common indicator of oxidative stress, was assessed by measuring TBARS, using a modified procedure (43) of the general protocol (38).

Data analysis. In all experiments except the ESR studies, statistical analyses were performed with Statview software (SAS Institute), using the chi-square (χ^2) or unpaired Student's *t* test, Kaplan-Meier survival analysis, or the nonparametric Mann-Whitney U test when appropriate. All values are reported as means ± SEs. *P* values of <0.05 were considered significant. For the ESR studies, statistical analysis was performed by one-way ANOVA. When *P* was <0.01, ANOVA was followed by a Newman-Keuls multiple-comparison test for intergroup differences, which were considered significant when *P* was <0.05. Values are reported as means ± SDs.

RESULTS

Targeted disruption of the *Trp53inp1* gene results in a null mutation. To investigate the physiological function of *Trp53inp1*, we generated *Trp53inp1*-deficient mice by gene targeting. Briefly, a null mutation was introduced in 129/Sv ES cells by replacing coding exons 2, 3, and 4 of the *Trp53inp1* gene with a neomycin resistance cassette (Fig. 1A). Germ line transmission was obtained for one of the two recombinant ES clones injected into host C57BL/6 blastocysts: the progeny did not carry the selection cassette. We intercrossed these heterozygous mutants (*Trp53inp1*$^{+/-}$), and DNA from the tails of the resulting littermates was analyzed by PCR (Fig. 1B). The three genotypes (*Trp53inp1*$^{+/+}$, *Trp53inp1*$^{+/-}$, and *Trp53inp1*$^{-/-}$) were represented according to the principles of Mendelian inheritance. Absence of gene expression in *Trp53inp1*$^{-/-}$ mice was confirmed by RT-PCR on RNA from the spleen (Fig. 1C) and by Western blotting on protein lysates from embryonic fibroblasts (Fig. 1D), confirming transmission of the null mutation. *Trp53inp1*$^{-/-}$ mice are viable and fertile and show no gross developmental or morphological abnormalities. Histological analyses of several organs, including the pancreas, liver, lung, spleen, kidney, heart, and colon from adult mice were performed and revealed no obvious abnormalities (data not shown). *Trp53inp1*-deficient mice were monitored for up to 2 years, and no spontaneous tumor has been observed so far.

Mice deficient in *Trp53inp1* are more sensitive to induced colon tumorigenesis associated with chronic inflammation. Susceptibility to tumorigenesis was tested, using the colitis-associated cancer model induced by a single injection of AOM followed by repeated cycles of DSS ingestion, as previously described (17). We treated groups of WT and *Trp53inp1*-deficient littermates ($n = 31$ and 36, respectively). The mice were sacrificed at 9 weeks after being injected with AOM, and the colons were assessed for the presence of tumors. Tumors were counted on high-resolution photographs of the colons (Fig. 2A). The incidence of macroscopic tumors was higher for *Trp53inp1*-deficient mice than for WT mice: 33 out of 36 (91.7%) mice deficient for *Trp53inp1* had gross tumors, versus 19 out of 31 (61.3%; $P < 0.05$) WT mice. The number of tumors per mouse (multiplicity) was twofold higher in *Trp53inp1*-deficient mice than in WT mice (Fig. 2B). We also calculated the weight-to-length ratios of the colons and compared them with those from untreated animals as an estimation of tumoral mass. In untreated animals of both genotypes, this

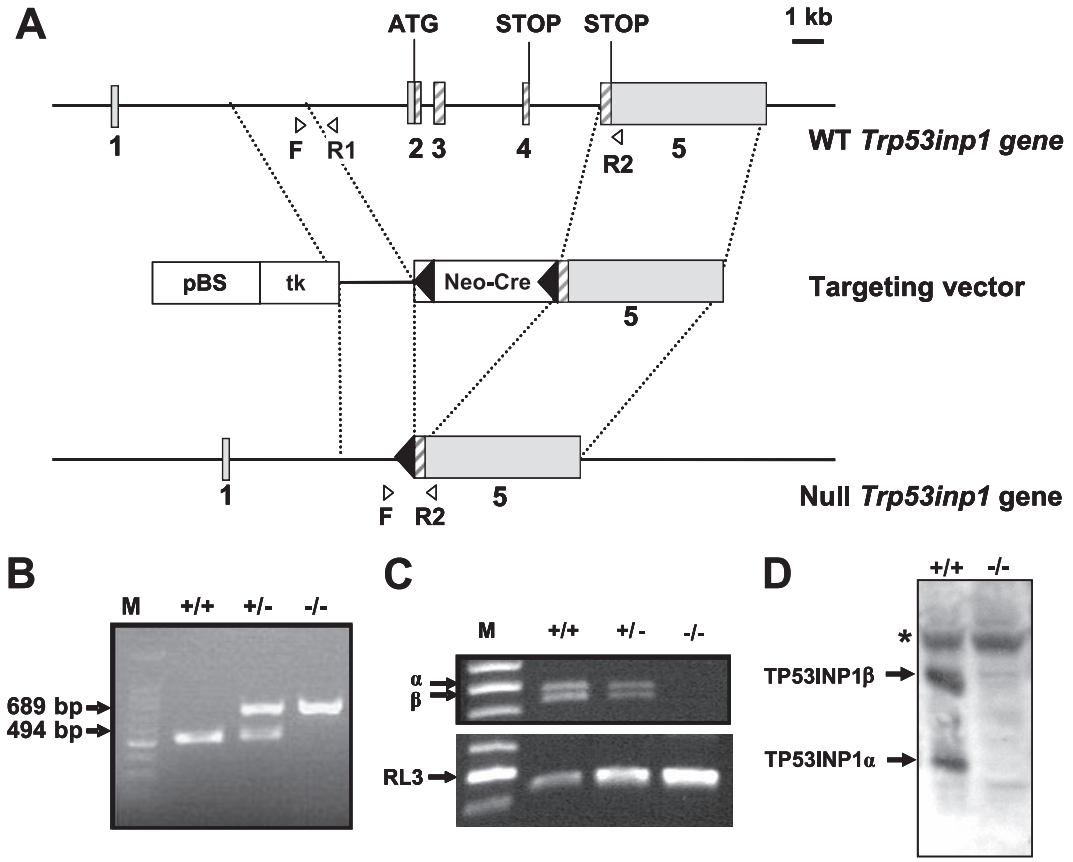

FIG. 1. Inactivation of the *Trp53inp1* gene in mice. (A) Targeting strategy. The endogenous *Trp53inp1* locus (WT, top bar), targeting construct (middle bar), and targeted *Trp53inp1* locus (bottom bar) are shown schematically. The five exons of *Trp53inp1* are represented by gray boxes, and the coding regions are hatched. The translation initiation codon located in the second exon and the stop codons located in the fourth and last exon are depicted. In the targeting vector, the boxes correspond to the *loxP*-flanked (black arrowheads) Neo-Cre cassette containing the neomycin resistance gene and the Cre recombinase gene under the control of the testes-specific angiotensin-converting enzyme gene promoter (Neo-Cre), the thymidine kinase expression cassette (tk), and the pBlueScript II KS^+ vector (pBS). The F, R1, and R2 primers used to detect the two alleles are indicated by the white arrowheads. (B) PCR analysis of DNA obtained from the tails of WT (+/+) mice and their littermates heterozygous (+/−) and homozygous (−/−) for the *Trp53inp1* deletion. The primers F, R1, and R2 were used in the same amplification reaction. M, molecular size marker (in base pairs). (C) RT-PCR analysis. Total RNA from the spleens of $Trp53inp1^{+/+}$, $Trp53inp1^{+/-}$, and $Trp53inp1^{-/-}$ mice was analyzed by RT-PCR with primers for *Trp53inp1* (identifying the two transcripts generated by differential splicing of exon 4) or primers for RL-3 as the housekeeping-gene control. (D) Western blot analysis. Lysates (60 μg protein/lane) from H_2O_2-treated $Trp53inp1^{+/+}$ and $Trp53inp1^{-/-}$ mouse embryonic fibroblasts were analyzed by immunoblotting, using an in-house rat monoclonal antibody directed against both isoforms of TP53INP1. The asterisk indicates a nonspecific band.

ratio was remarkably constant, around 2 mg/mm (Fig. 2C). In AOM-DSS-treated animals, the weight-to-length ratio was increased significantly relative to that for untreated animals, but the weight gain was twofold higher in *Trp53inp1*-deficient animals (4.7 ± 0.4 mg/mm) than in WT animals (3.3 ± 0.2 mg/mm; $P < 0.01$). Microscopic analyses of H&E-stained sections showed that the tumors in both groups were colonic adenomas with a high grade of dysplasia (Fig. 2F to I). Glands were atypical and densely packed, with many mitotic figures. No case of infiltrative colonic carcinoma was noted. The mean tumor surface was measured and shown to be similar for those from *Trp53inp1*-deficient and WT colons (Fig. 2J). Proliferation and apoptosis in the tumors were assessed by PCNA and active caspase-3 immunostaining, respectively (Fig. 2K and L). Both the proliferation and apoptosis indices were shown to be slightly higher for tumors from *Trp53inp1*-deficient animals than for those from WT mice, but those differences were not statistically significant. Taken together, our results indicate that TP53INP1 is essential for protection from colitis-associated cancer.

Finally, the development of tumors was assessed for mice either treated with a single injection of AOM without further DSS treatment or mock-injected with PBS and then treated with three cycles of DSS. The mice were sacrificed at 9 weeks after injection, corresponding to the timeline of the AOM-DSS protocol, or at 7 months, to assess the long-term effects of both treatments (Table 2). At 9 weeks, neither WT nor *Trp53inp1*-deficient mice had developed tumors. WT mice did not develop tumors at 7 months after treatment. On the other hand, for the *Trp53inp1*-deficient mice, AOM or DSS alone was sufficient to induce tumor development in a few animals after 7 months.

Mice deficient in *Trp53inp1* are more sensitive to DSS-induced acute colitis. In order to determine whether a more-

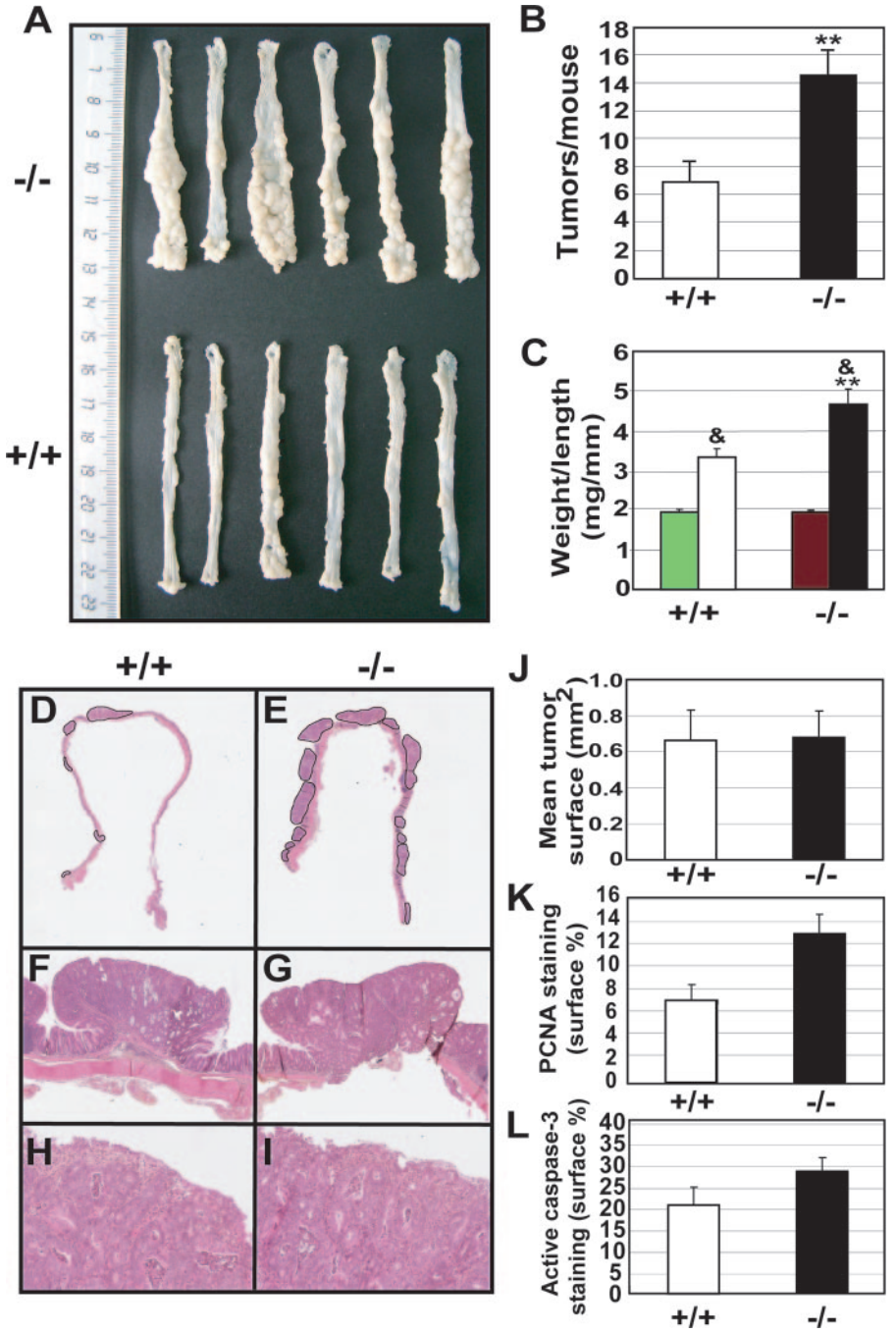

FIG. 2. Absence of *Trp53inp1* increases colon tumorigenesis. Cohorts of 7- to 10-week-old WT and *Trp53inp1*-deficient mice (n = 31 and 36, respectively) were treated with a single injection of AOM, followed by three cycles of DSS to induce a moderate, long-lasting colitis. Animals were sacrificed 9 weeks after injection of AOM, and the colons were collected and analyzed for the presence of tumors. (A) Representative macroscopic images of colons from *Trp53inp1*-deficient (−/−) and WT (+/+) animals. (B) Mean number ± SE of tumors per colon from WT and *Trp53inp1*-deficient animals (**, $P < 0.01$ versus results for the WT). (C) Means ± SEs of the weight-to-length ratios of the colons. The green and red bars correspond to WT and *Trp53inp1*-deficient untreated animals, respectively (&, $P < 0.01$ versus results for untreated mice; **, $P < 0.01$ versus results for the WT). (D and E) Overview of H&E-stained sections of representative colons from WT (left) and *Trp53inp1*-deficient mice (right). The tumors are encircled. Microscopic examination of the tumor sections was performed at ×25 (F and G) or ×200 (H and I) magnification. (J) Mean tumor surface ± SE measured on one colon section for each animal. (K and L) Tumor proliferation and apoptosis indices determined by PCNA and active caspase-3 staining, respectively, and expressed as the percentage of the total tumoral surface stained ± the SE.

severe colitis could account for the increased tumorigenesis in *Trp53inp1*-deficient mice, we induced acute colitis in mice by administering 3.5% DSS in their drinking water for 7 days, after which they received tap water only (without DSS) until they were sacrificed. The mice were monitored for 15 days after being treated with DSS for weight loss, DAI, and survival. Weight loss in both groups of mice became significant from day 7 onward (Fig. 3A). Weight loss for the WT mice reached a

TABLE 2. Incidence of tumors in the colons of mice treated with either AOM alone or DSS alone, at 9 weeks or 7 months

Treatment	Time since treatment	Incidence for mice with or without *Trp53inp1*:[a]	
		+/+	−/−
AOM alone	9 wk	0/6	0/6
	7 mo	0/8	1/5
DSS alone	9 wk	0/6	0/6
	7 mo	0/7	2/7

[a] The incidence of tumors is reported as the ratio of tumor-bearing mice to the total number of mice. +/+, mice with the *Trp53inp1* gene; −/−, mice without the *Trp53inp1* gene.

maximum of 10% around day 11, followed by a complete recovery at day 14. In *Trp53inp1*-deficient mice, weight loss was much more severe, with a maximum loss of 25% at day 12, and recovery was incomplete, since the mice were still 20% below their initial weight at day 15. Colitis in WT animals did not induce significant mortality, and their survival rate at day 15 was above 90% (Fig. 3B). On the other hand, DSS treatment of *Trp53inp1*-deficient animals resulted in a very high mortality rate: less than 50% of the animals survived to day 15 ($P < 0.05$) (Fig. 3B). Monitoring of survival was prolonged up to 1 month, and the survival curve did not change after day 15 (data not shown). Analysis of the DAIs showed that clinical signs of disease were already present at day 3 in *Trp53inp1*-deficient mice, while WT mice were still healthy at that time (Fig. 3C). The DAI progressed rapidly in *Trp53inp1*-deficient animals and reached a global twofold increase compared to that of the WT at day 8. Finally, histological analyses were performed to assess tissue damage. At day 3 of treatment, there were no histological abnormalities (data not shown). Analyses at day 9 showed that mucosal ulcerations were more severe in the co-

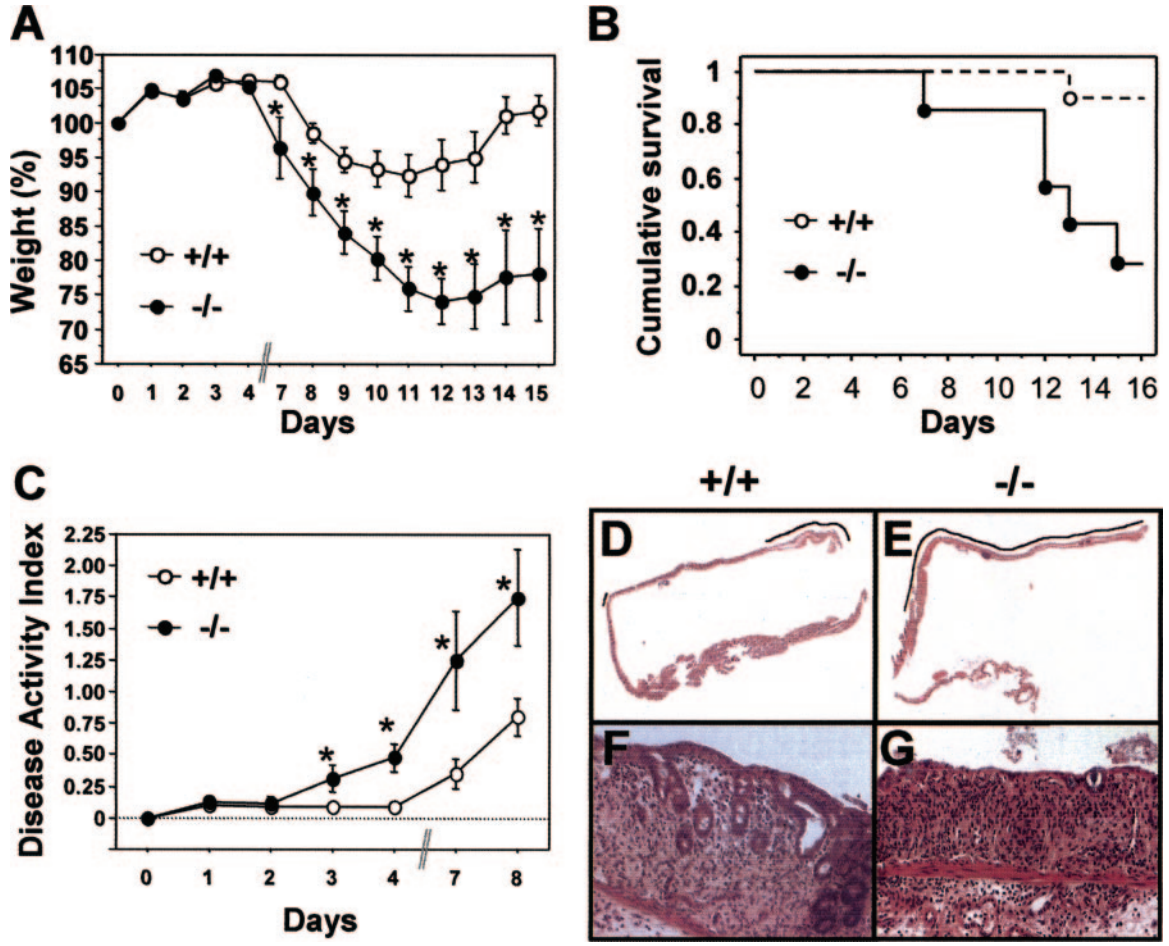

FIG. 3. The absence of *Trp53inp1* increases the severity of colitis in mice. Cohorts of 7- to 10-week-old mice ($n > 12$ per group) were given 3.5% DSS in their drinking water for 7 days to induce acute colitis and then given tap water without DSS while being monitored for 15 days. (A) The mice were weighed every day, and the values were expressed as percentages of the initial weights. Mice deficient in *Trp53inp1* lost more weight and showed poorer recovery than WT mice. (B) Kaplan-Meier analysis showed a higher mortality rate after induction of colitis in the *Trp53inp1*-deficient mice than in the WT mice ($P = 0.029$). (C) The DAI increased more rapidly, and to higher values, in *Trp53inp1*-deficient mice than in WT mice. The data shown in panels A, B, and C are representative of two independent experiments. For panels A and C, an asterisk indicates a P value of <0.05 for *Trp53inp1*-deficient mice (−/−) versus that for WT mice (+/+). (D and E) Microscopic examination of colon sections at 9 days after the induction of colitis shows more-extensive ulceration (indicated by the black line) in *Trp53inp1*-deficient animals (right) than in the WT (left). (F and G) Histological analysis at higher magnification (×200) shows moderate epithelium damage in WT mice, with a progressive disappearance of glands (left). The damage is more severe in *Trp53inp1*-deficient animals, where only the surface epithelium persists (G).

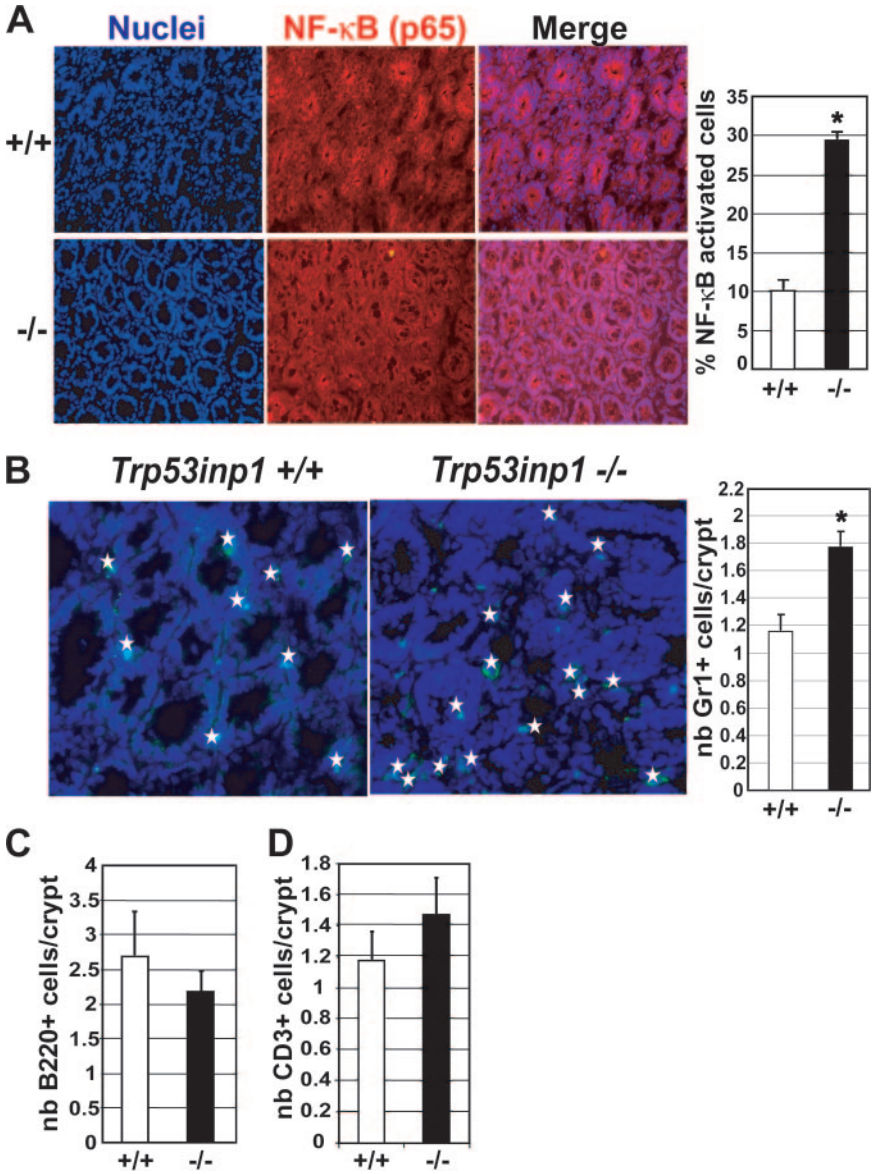

FIG. 4. The absence of *Trp53inp1* increases epithelial cell NF-κB activation and granulocyte infiltration during acute colitis. Colon cryosections (10 μm) were obtained from WT and *Trp53inp1*-deficient animals ($n = 3$ of each genotype) after 10 days of colitis. (A) Nuclei stained with Hoechst (blue) are shown on the left; the middle panel shows NF-κB-stained (red) colon sections with a p65-specific antibody (magnification, ×40). The histogram on the right shows the quantification of NF-κB activation expressed as the mean percentage (± SE) of NF-κB-positive nuclei of the total number of nuclei. (B) Gr1-stained (green) colon sections (magnification, ×60) are shown; positive cells are highlighted with a star. The histogram on the right shows the quantification of Gr1-positive cells per crypt expressed as means ± SEs. (C and D) Colon-infiltrating B and T lymphocytes were stained, using B220- and CD3ε-specific antibodies, respectively. The results were quantified and expressed as for panel B. *, $P < 0.05$ for *Trp53inp1*-deficient mice (−/−) versus results for the WT (+/+). nb, number.

lons of *Trp53inp1*-deficient mice than in those of WT mice (Fig. 3D to G), with crypt damage scores of 10.2 ± 0.93 and 8.0 ± 0.97, respectively ($P < 0.05$). Taken together, these results show that *Trp53inp1*-deficient mice are more susceptible to experimental acute colitis, which might be related to the increased susceptibility of these mice to induced colorectal cancer.

Inflammation is exacerbated in *Trp53inp1*-deficient mice during DSS-induced acute colitis. In order to determine whether a disorder in the inflammatory process could account for a more-severe colitis in *Trp53inp1*-deficient mice, we analyzed both NF-κB activation and immune cell infiltration in the colonic epithelia during colitis. NF-κB is a proinflammatory transcription factor which, upon activation, induces transcription of genes involved in survival, proliferation, inflammation, and innate immunity. Inactive NF-κB is present in the cytoplasms of all cells and is translocated to the nucleus upon activation. We assessed NF-κB activation in colons from WT and *Trp53inp1*-deficient mice at day 10 of colitis by immunohistofluorescence, using an antibody specific for the p65 subunit of NF-κB (Fig. 4A). Our results showed a threefold-higher percentage of NF-κB-positive nuclei in colons from *Trp53inp1*-

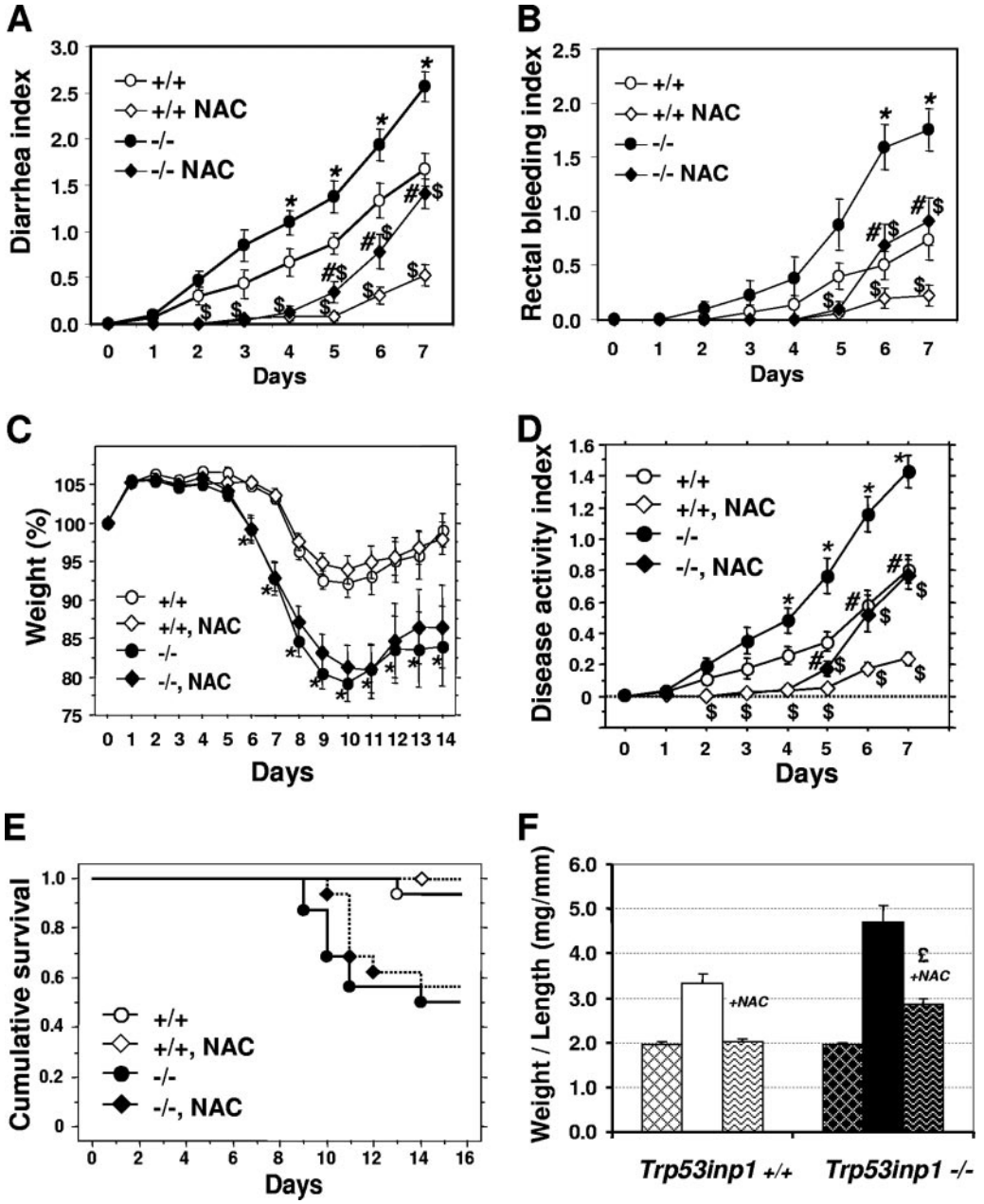

FIG. 5. (A to E) Treatment with NAC abolishes genotype-specific differences in early colitis. Cohorts of WT (+/+) or *Trp53inp1*-deficient mice (−/−) (n = 15 to 18 mice per group) were treated with DSS with or without cotreatment with NAC. The incidences of the clinical signs of pathology (diarrhea, rectal bleeding, and weight loss) are shown in panels A to C. Panel D shows the averages of the three values from panels A to C (the DAI). *, $P < 0.05$ for *Trp53inp1*-deficient mice not treated with NAC versus results for untreated WT mice; $, $P < 0.05$ for NAC-treated mice versus results for mice of the same genotype not treated with NAC; #, $P < 0.05$ for NAC-treated *Trp53inp1*-deficient mice versus results for NAC-treated WT mice. Administration of NAC significantly delays diarrhea and rectal bleeding in both genotypes. After day 5 of treatment, genotype-specific differences were observed again, as disease progression was more rapid in *Trp53inp1*-deficient animals than in WT mice. For both groups, administration of NAC does not significantly reduce colitis-induced weight loss or mortality, as shown by Kaplan-Meier analyses (E). (F) AOM-DSS-induced colon tumorigenesis in the presence of NAC. The weight-to-length ratio of the colons from mice given NAC in their drinking water during the whole AOM-DSS procedure (wave-patterned bars) shows that NAC almost completely abolishes tumorigenesis in WT mice, whereas it only reduces tumorigenesis in *Trp53inp1*-deficient mice (£, $P < 0.01$ for AOM-DSS-plus-NAC-treated mice compared to the results for untreated mice). The ratios shown in Fig. 2C are reported here for easy comparison (hatched bars correspond to untreated animals).

deficient mice than in those from WT colons. Thus, NF-κB activation is stronger in colons from *Trp53inp1*-deficient mice than in those from WT mice. Then we analyzed immune cell infiltration at day 10 of colitis by immunohistofluorescence, using antibodies specific for markers of either innate immune cells (Gr1 marker for granulocytes) or adaptive immune cells (B220 and CD3ε markers for B and T cells, respectively). Quantification of the ratio of positive cells to the number of

colonic crypts showed a higher infiltration of Gr1-positive cells in colons from *Trp53inp1*-deficient mice than in those from WT mice (Fig. 4B), whereas the degrees of B- and T-cell infiltration did not differ (Fig. 4C and D). Altogether, these results indicate that *Trp53inp1*-deficient mice developed a stronger inflammatory response than their WT counterparts following DSS treatment, which is in accordance with their increased susceptibility to experimental acute colitis.

Reduction of colitis by treatment with NAC. It has been shown that IBD is associated with oxidative stress, potentially through production of ROS, which include a variety of molecules derived from molecular oxygen, such as H_2O_2 and the free radicals $O_2^{\cdot -}$ and $HO^{\cdot}$. Both accumulation of H_2O_2 produced by colonic epithelial cells and release of $O_2^{\cdot -}$ by infiltrating granulocytes and macrophages occur during colitis (33, 45, 52). As *Trp53inp1* expression is induced by oxidative stress (H_2O_2 and ionizing radiation), we tested whether *Trp53inp1* deficiency could result in increased oxidative load in *Trp53inp1*-deficient mice, which might cause a more-severe colitis and subsequent colorectal carcinogenesis. For this purpose, we compared the effects of antioxidant treatment on acute colitis in *Trp53inp1*-deficient and WT mice. Given the protective effect of NAC on experimental colitis (1) and colitis-associated colorectal adenocarcinoma (51), mice were given NAC from 10 days before the start of DSS treatment and continuously until the end of the protocol. Treatment with NAC significantly delayed diarrhea and rectal bleeding (which are early clinical signs of colitis) in mice of both genotypes (Fig. 5A and 5B), but no significant differences in weight loss (which is a later clinical sign of colitis) and mortality were seen (Fig. 5C and E). Detailed analyses of the DAIs (Fig. 5D) show a first phase (from day 0 to 4), during which NAC treatment completely abolished the clinical signs of colitis, and a second phase, during which the DAI started to increase while remaining significantly lower than for untreated mice. This second phase became significant at day 5 for *Trp53inp1*-deficient mice, whereas it was delayed to day 6 in WT mice (Fig. 5D). In this second phase, the pathology was significantly more severe in *Trp53inp1*-deficient mice than in the WT, as was observed in the absence of NAC treatment.

Finally, we tested whether NAC could inhibit development of tumors induced by AOM-DSS treatment. Our data (Fig. 5F) show that tumorigenesis is almost completely abolished in NAC-treated WT mice. On the other hand, NAC-treated *Trp53inp1*-deficient mice still developed tumors, although less often than did *Trp53inp1*-deficient mice that were not treated with NAC.

***Trp53inp1*-deficient mice show increased plasma and colon oxidative stress.** Since it allows direct detection and characterization of free radicals, ESR spectroscopy can provide the most-definitive proof of the formation of ROS after the induction of acute colitis in *Trp53inp1*-deficient animals compared to that in the WT. It is believed that blood serum and plasma antioxidant levels reflect the total antioxidant capacity of the body. Decreased plasma levels of ascorbate (vitamin C), which is one of the main water-soluble antioxidants, is observed during human IBD (27). Addition of DMSO to the blood plasma from both WT and *Trp53inp1*-deficient animals led to the detection of the AFR-ESR doublet ($a_H = 0.18$ mT) (Fig. 6A and B). We have previously shown that the concentration of this AFR-DMSO complex is representative of the ascorbate content of the plasma (42, 44). In untreated WT mice, the baseline AFR-DMSO concentration corresponded to the signal yielded by 40 to 50 μM sodium ascorbate (Fig. 6C). In contrast, *Trp53inp1*-deficient mice exhibited a significantly decreased AFR-DMSO content (−50% versus that of the baseline concentration) (Fig. 6B and C), suggesting that these animals are continuously subjected to free-radical-induced oxidative stress that causes ascorbate consumption in the plasma. Induction of acute colitis strongly depleted AFR-DMSO levels in the plasma at day 2 for WT (−62% versus those for the baseline) and *Trp53inp1*-deficient (−71% versus those for untreated *Trp53inp1*-deficient animals) mice (Fig. 6C). As expected, these *Trp53inp1* deficiency- or acute colitis-induced ascorbate depletions occurred along with a significant increase in lipid peroxidation levels in the plasma both in DSS-treated versus untreated groups and in *Trp53inp1*-deficient versus WT animals (Fig. 6D). Interestingly, we noted a higher lipid peroxidation level in untreated *Trp53inp1*-deficient mice than in DSS-treated WT animals (Fig. 6D).

To shed light on the nature of the free radicals responsible for the above-described disorder of ascorbate consumption and lipid peroxidation in the plasma of *Trp53inp1*-deficient mice and to establish a link between this oxidant stress and the susceptibility of *Trp53inp1*-deficient mice to experimental acute colitis, spin-trapping experiments were undertaken on cultured colons, using DEPMPO nitrone as the spin trap. Short-lived free radicals, such as those formed in biological systems, add to nitrones to yield persistent ESR-detectable aminoxyl adducts, providing structural and quantitative information on the primary species formed. DEPMPO was chosen because its spin adducts with $O_2^{\cdot -}$ and $HO^{\cdot}$ (DEPMPO-OOH and DEPMPO-OH, respectively) are among the more stable and easily distinguishable by ESR (16). In culture supernatants from untreated WT and *Trp53inp1*-deficient colons, AFR signals were seen but not DEPMPO adducts (Fig. 7A and B). Direct observation of released AFR has been made previously in cases of oxidative stress and it can be considered an indicator of tissue damage (42) and/or of the interaction of ascorbate with free radicals (4). Figure 7C shows that the levels of AFR released in culture supernatants by samples from untreated *Trp53inp1*-deficient mice were about threefold higher than those from WT mice ($P < 0.05$; $n = 4$). In spin trap-added colon cultures from mice submitted to DSS-induced colitis for 2 days, strong DEPMPO aminoxyl ESR signals were detected for *Trp53inp1*-deficient mice and, to a lesser extent, for WT animals (Fig. 7A, B, and D). Computer simulations of these signals revealed three components having the following splitting constants (in mT): DEPMPO-OH ($a_N = 1.450$; $a_P = 4.729$; $a_H = 1.347$), which provides an eight-line signal, and two DEPMPO-alkyl adducts, ranging from 25 to 79% of the total signal and having sets of parameters ($a_N = 1.472$ (1.470); $a_P = 4.855$ (4.710); $a_H = 2.153$ [2.080]) close enough to give a global signal having the appearance of a single eight-line spectrum. When SOD was added to the spin trap-containing media, complete inhibition of DEPMPO adduct formation was observed (Fig. 7A and B), demonstrating a common $O_2^{\cdot -}$ origin for the aminoxyl signals. In SOD experiments, AFR signals were still detected, the intensities for deficient mice being again threefold higher than for WT animals (Fig. 7C). In colons from

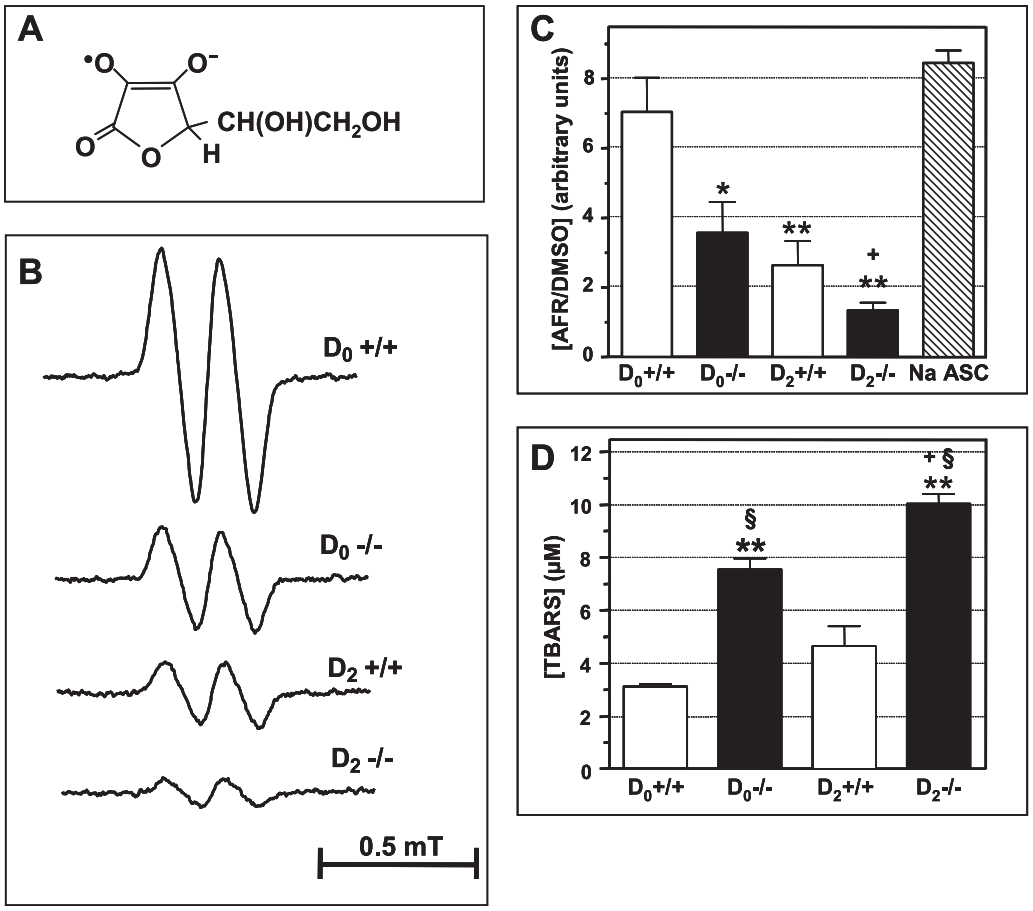

FIG. 6. *Trp53inp1* deficiency decreases ascorbate levels in plasma, increases lipid peroxide content in plasma, and potentiates acute colitis-induced depletion of ascorbate and lipid peroxidation in plasma. Acute colitis was induced in WT (+/+) and *Trp53inp1*-deficient (−/−) mice by treatment with 3.5% DSS for 2 days (D_2). D_0 indicates samples from untreated animals. Ascorbate levels in plasma were assessed through ESR detection of AFR-DMSO doublets, and lipid peroxidation levels were determined by TBARS assay. (A) Chemical structure of AFR. (B) Selected ESR spectra from WT and *Trp53inp1*-deficient mice either untreated or treated for 2 days with DSS. (C) Means ± SDs (n = 5 to 7 mice per group) of AFR-DMSO concentrations in plasma from the different groups of animals calibrated to a similar signal yielded by 50 μM aqueous sodium ascorbate. (D) Means ± SDs (n = 5 to 7 mice per group) of TBARS concentrations in plasma. Untreated *Trp53inp1*-deficient mice show significantly decreased ascorbate levels in plasma and increased lipid peroxide concentrations compared to those of untreated WT mice. *Trp53inp1*-deficient mice are more susceptible than WT mice to acute colitis-induced ascorbate depletion and increased lipid peroxidation in the plasma. The statistics are based on the results of one-way ANOVA ($P < 0.0002$) followed by Newman-Keuls tests for intergroup differences. *, $P < 0.01$; **, $P < 0.001$ versus results for $D_0^{+/+}$; §, $P < 0.001$ versus results for $D_2^{+/+}$; +, $P < 0.05$ versus results for $D_0^{-/-}$.

treated WT and *Trp53inp1*-deficient mice, addition of CAT decreased DEPMPO adduct formation by only 60% (Fig. 7D), yet implying that there was H_2O_2 in the ESR signal formation. Incubating 10 mM aqueous DEPMPO with 3.5% DSS at 25°C for up to 6 h yielded a low stationary level of DEPMPO-OH (<1% of the weakest signal detected from treated WT colons; data not shown), indicating a slow thermal decomposition that is common to nitrones. Consequently, no significant aminoxyl formation unrelated to radical trapping is likely to occur, since only traces of DSS, if any, could be in contact with DEPMPO in our study.

DISCUSSION

We hypothesized that the gene encoding the stress protein TP53INP1 could influence inflammation-associated tumorigenesis, since it could act as a tumor suppressor. Indeed, (i) the *TP53INP1* gene is induced by p53, (ii) TP53INP1 interacts with p53 and increases its *trans*-activation activity, (iii) *TP53* (encoding p53) is a tumor suppressor gene, (iv) TP53INP1 has antiproliferative and proapoptotic activities when overexpressed, and (v) TP53INP1 is down-regulated in gastric cancer (23) and in colorectal and pancreatic carcinomas (our unpublished data). Therefore, we generated mice in which the *Trp53inp1* gene is inactivated. We confirmed the absence of *Trp53inp1* expression in animals homozygous for the deficiency. These animals are apparently healthy, and they have not developed spontaneous tumors nor colitis so far.

We investigated the role of *Trp53inp1* in inflammation-associated colonic tumor development by evaluating the susceptibility of *Trp53inp1*-deficient and control WT mice to developing tumors during a protocol of colorectal tumorigenesis in which one injection of the procarcinogen AOM was followed by repeated administrations of DSS leading to chronic colon

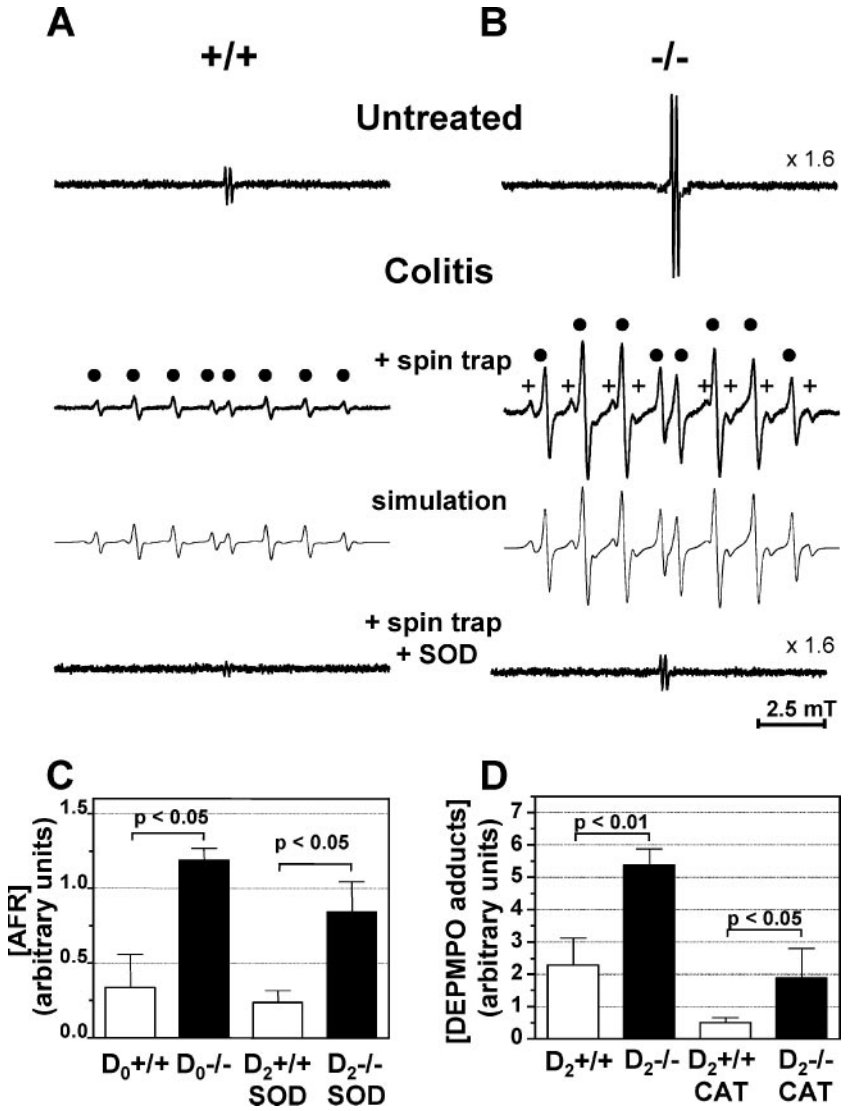

FIG. 7. Colons from *Trp53inp1*-deficient mice behave as continuous, low-level ROS-producing systems which are stimulated by acute colitis. ROS production was assessed by ESR using spin trap DEPMPO, in the presence or absence of 100 U/ml SOD or 5,000 U/ml CAT in the culture media of colons from WT or *Trp53inp1*-deficient mice either untreated or treated for 2 days with 3.5% DSS. (A and B) Representative spectra from WT (+/+) and *Trp53inp1*-deficient mice (−/−), respectively. In panels A and B, the computer-simulated spectra are presented below the experimental spectra, while filled circles and pluses mark the lines from DEPMPO-OH and DEPMPO-alkyl adducts, respectively. The *y* axis scales for the top and bottom AFR spectra are given relative to the middle DEPMPO adduct signals. The bottom spectra in panels A and B show the complete inhibition of these DEPMPO adduct signals by SOD. (C) Means ± SDs ($n = 4$) of the concentrations of AFR in supernatants. (D) Means ± SDs ($n = 4$) of the relative total spin adduct concentrations. The histogram in panel C shows that *Trp53inp1* deficiency ($D_0^{-/-}$) significantly amplifies low-level background, ROS-triggered AFR release observed in the colons of untreated WT mice. AFR release can be evidenced in colitic colons due to the complete inhibition of spin-trapping signals by SOD. The histogram in panel D shows that acute colitis induces a burst of DEPMPO-trapped radicals ($HO^{\cdot}$ and alkyl radicals) in colon cultures which is significantly stronger in *Trp53inp1*-deficient mice. Spin adduct formation is partially inhibited by the addition of CAT. The statistics are based on one-way ANOVA ($P < 0.007$) followed by the Newman-Keuls test for intergroup differences (level of significance, $P < 0.05$). $D_0^{+/+}$, untreated WT mice; $D_0^{-/-}$, untreated *Trp53inp1*-deficient mice; $D_2^{+/+}$, WT mice treated for 2 days with DSS; $D_2^{-/-}$, *Trp53inp1*-deficient mice treated for 2 days with DSS.

inflammation. We observed a significantly higher rate of both tumor incidence and multiplicity for *Trp53inp1*-deficient mice than for their WT counterparts. The increase in colon weight was twofold higher in *Trp53inp1*-deficient mice than in WT mice, reflecting the twofold-higher number of tumors. This increase was independent of the proliferation and death of tumoral cells, since proliferation and caspase-3 activation indices for tumors were not significantly different between the two genotypes, in agreement with the observation that tumors were of the same size in both genotypes. Interestingly, when we investigated tumor development induced either by AOM injection alone or by DSS-induced chronic colitis without prior injection of AOM, we observed tumors only in *Trp53inp1*-deficient mice during examinations 7 months after starting the experiment. Deficiency of TP53INP1 is thus an enhancing factor for colorectal tumorigenesis induced by either chemical

carcinogen treatment alone or by chronic inflammation alone. Altogether, our data showed that the absence of TP53INP1 significantly exacerbates tumor development, suggesting that early events in tumoral transformation (initiation) in epithelial cells were different in the two groups. Alternatively, absence of TP53INP1 might promote tumorigenesis by favoring clonal expansion of initiated cells. Considering that the *Trp53inp1* gene is induced by cell stress, that it is highly expressed in immune cells (7; also unpublished data), and that an association between inflammation and cancer has been well documented, we favor the latter possibility.

In order to test the hypothesis that TP53INP1 has a physiological role in colonic inflammation, we challenged mutant and WT mice to acute DSS-induced colitis. The *Trp53inp1*-deficient mice lost much more weight than the WT mice, and they failed to recover their initial weights by day 15 of the experiment. The other clinical signs of colitis, namely diarrhea and rectal bleeding, were consistently more severe in *Trp53inp1*-deficient mice. Eventually, in the course of the experiment, mortality was significantly higher among *Trp53inp1*-deficient mice. Taken together, these data show that DSS-induced colitis is particularly severe in *Trp53inp1*-deficient mice, suggesting that TP53INP1 plays a role in limiting colonic inflammation. Interestingly, we noted that the first 7 days of DSS treatment had no impact on the weight and survival of mice, the striking differences appearing later. However, clinical signs of pathology (diarrhea and rectal bleeding) appeared at day 3, although the histology remained normal. This is in agreement with the previously documented delay between loss of mucosal integrity (which contributes to diarrhea and bleeding) and the first histologically detectable lesions in the mouse model of DSS-induced colitis (30). Finally, histological analyses showed that mucosal damage was more severe in *Trp53inp1*-deficient colons than in those of the WT during colitis and was accompanied by increased infiltration by Gr1-positive cells and augmentation of the epithelial cell fraction containing activated NF-κB. These observations indicated exacerbated colon inflammation in *Trp53inp1*-deficient mice. The role of NF-κB in the initiation and promotion of tumorigenesis has been documented in many reports (recently reviewed in reference 26). NF-κB contributes to tumor development, acting as a protumoral factor, during colitis-associated colorectal cancer in both enterocytes and myeloid cells (17). Thus, increased NF-κB activation in *Trp53inp1*-deficient colonic epithelial cells during chronic colitis was likely involved in increased colorectal tumorigenesis.

Oxidative stress is a major risk factor associated with inflammation and carcinogenesis (21, 22, 45, 52). It arises from an imbalance between oxidants and antioxidants in favor of the former, leading to an overload of ROS and RNS, which causes DNA and protein oxidation and lipid peroxidation, which can in turn lead to alterations in cell turnover and cell death (15, 31, 33, 63). A low level of oxidative stress can stimulate cell division and thus the promotion of tumor growth. It is known that during acute and chronic inflammation, ROS are produced at rates that overwhelm the capacity of the endogenous defense system to remove them (33, 49). To get further insights into the physiological role of TP53INP1 during oxidative stress in the colon, we evaluated the impact of an antioxidant during both acute colitis and colitis-associated tumorigenesis in mutant and WT mice. NAC is a precursor of reduced glutathione, a major antioxidant in the cells, and may also scavenge ROS on its own (12, 51). We observed a preventive effect of NAC on colitis during the first days of DSS treatment in cohorts of both genotypes, confirming the major role played by oxidative stress during DSS-induced acute colitis. Nevertheless, we evidenced a second phase during which the preventive action of NAC was less efficient in *Trp53inp1*-deficient mice than in WT mice, as the former showed clinical signs of colitis sooner. In addition, NAC efficiently prevented tumor development in WT mice but not in *Trp53inp1*-deficient mice, which still presented significant adenoma development. These results indicate that, as DSS treatment progresses, administered NAC becomes unable to inhibit colitis pathology. Although we do not exclude the possibility that a ROS-independent mechanism may be implicated in the second phase of colitis progression, one can hypothesize that either the level or the nature of ROS generated in the inflamed colons hinders the capacity of NAC to remove them. If we assume that the latter hypothesis is correct, *Trp53inp1*-deficient mice should present higher ROS levels in the colon than WT mice, as they develop a more-severe colitis.

We assessed this question directly, using the powerful ESR technology. It has been shown that ascorbate depletion or its reaction with free radicals can be directly probed by direct detection of AFR-DMSO or AFR, respectively, in a variety of chronic or acute oxidative stress situations in animals (28, 29, 42) and humans (2, 43, 44). Altered ascorbic acid status has been reported in the mucosa (5) and plasma (27) of IBD patients. By documenting a decrease in AFR-DMSO in DSS-treated WT mice, our data confirm the usefulness of this ESR index in the measurement of ascorbate levels. Thus, our parallel finding that induction of acute colitis results in even more depleted ascorbate levels and elevated lipid peroxidation status in *Trp53inp1*-deficient mice than in their WT counterparts strongly advocates for higher production of ROS in the former. In this regard, low basal levels of ascorbate and high concentrations of lipid peroxidation in plasma from untreated *Trp53inp1*-deficient mice demonstrate that these animals are submitted to chronic oxidant stress that could explain their increased ROS production during colitis. Unexpectedly, whereas untreated deficient mice showed an even higher mean TBARS concentration than WT mice during colitis, the difference between genotypes was no longer significant for AFR-DMSO. Finally, the above data are in line with the appearance of a higher level of AFR released by the colons of untreated *Trp53inp1*-deficient animals, indicating more-severe tissue damage (44). Altogether, our results show that *Trp53inp1*-deficient mice present increased oxidative stress and reduced antioxidant defenses (at least regarding the ascorbate pool) in the absence of treatment compared to WT mice and that this stress is amplified during DSS-induced colitis, unequivocally pointing to a role for TP53INP1 in the control of the oxidative status in vivo.

Unstable free radicals involved in oxidative stress, such as $O_2^{\cdot -}$ and $HO^{\cdot}$, require a trapping reaction to be detected by ESR, but even with the use of an improved nitrone such as DEPMPO (16), the resulting aminoxyls are prone to unavoidable reduction to ESR-silent hydroxylamines, especially by ascorbate (50) or AFR, and/or to structural modification in biological systems. Thus, it is possible that some spin adduct

formation in colons from untreated *Trp53inp1*-deficient mice may have escaped from ESR detection due to the concomitant strong AFR release. We have previously reported that DEPMPO-OOH, the ESR spectrum of which displays 12 lines, can be readily converted to DEPMPO-OH by specific hydroperoxide-reducing enzymes such as glutathione peroxidase (16). This can explain why the DEPMPO-OH signals seen in DSS-treated mice can be completely inhibited by SOD, and we therefore demonstrate here that $O_2^{\cdot -}$ is the major, primary ROS formed in DSS-treated colons. The presence of an increased amount of superoxide in colons from *Trp53inp1*-deficient mice compared to that in colons from WT mice may be a consequence of the increased granulocyte infiltration observed in the former. Superoxide has been linked to the onset of DSS-induced colitis (32), and mechanisms of formation involving vitamin K semiquinones or specific enzymes such as xanthine oxidase have been proposed (9, 62). In our study, the observation of DEPMPO-alkyl adducts, likely secondary adducts of carbon-centered radicals, supports a decisive role for $HO^{\cdot}$, and its precursor, H_2O_2, as the actual damaging species. The poorer capacity of CAT to inhibit DEPMPO adduct formation in colon cultures from 2-days colitic *Trp53inp1*-deficient mice versus that for WT mice may reflect a higher capacity of the former to produce H_2O_2. The formation of $HO^{\cdot}$ in DSS-induced colitis has previously been hypothesized on the basis of more-indirect assays than ESR (8, 57).

To summarize, we would like to propose a model in which *Trp53inp1*-deficient mice deal with chronic endogenous oxidant stress by overconsuming endogenous antioxidant defenses (like blood ascorbate). While this compensation mechanism manages to prevent oxidative damage and related pathologies in the absence of exogenous challenge, it is insufficient to deal with strong oxidant stress during colitis, allowing extensive colon epithelium damage and concomitant leukocyte recruitment. Infiltrating $Gr1^+$ cells will release superoxide in the epithelium, thus increasing oxidative load and tissue damage. Whether TP53INP1 exerts an intrinsic or extrinsic function on granulocytes is currently being studied in the laboratory.

In conclusion, we showed that a deficiency in the *Trp53inp1* gene leads to increased tumorigenesis in the mouse model of AOM-DSS-induced colorectal cancer. Furthermore, *Trp53inp1*-deficient mice showed more-severe colitis than the WT, due to a higher oxidative load, which might account for enhanced tumoral promotion during colitis. These findings strengthen the hypothesis that TP53INP1 is a tumor suppressor and underscore the role of oxidative stress in colitis-associated cancer. In this work, we shed light on critical functions of TP53INP1 in the colon, which opens up new preventive and/or therapeutical avenues for the control of oxidative stress in IBD and CRC patients.

ACKNOWLEDGMENTS

We thank Anne Gillet for blastocyst injection and chimera breeding, Gilles Warcollier and the animal house staff for mouse care, Patricia Spoto for help in genotyping, Marie-Noëlle Lavaud for histological analyses, Patrice Berthézène for statistical analyses, and Jean-Charles Dagorn and Mathias Chamaillard for discussions.

This work was supported by INSERM, CNRS, the Association pour la Recherche sur le Cancer (B.M.), and Plate-forme RIO-MNG (B.M.). J.G. was supported by doctoral fellowships from the Ministère de l'Education Nationale de la Recherche et de la Technologie, the Association pour la Recherche sur le Cancer, and the Société Française du Cancer. C.C. was supported by a postdoctoral fellowship from the Association pour la Recherche sur le Cancer, and M.G. was supported by a postdoctoral fellowship from INSERM.

REFERENCES

1. **Ardite, E., M. Sans, J. Panes, F. J. Romero, J. M. Pique, and J. C. Fernandez-Checa.** 2000. Replenishment of glutathione levels improves mucosal function in experimental acute colitis. Lab. Investig. **80:**735–744.
2. **Bailey, D. M., S. Raman, J. McEneny, I. S. Young, K. L. Parham, D. A. Hullin, B. Davies, G. McKeeman, J. M. McCord, and M. H. Lewis.** 2006. Vitamin C prophylaxis promotes oxidative lipid damage during surgical ischemia-reperfusion. Free Radic. Biol. Med. **40:**591–600.
3. **Brachat, A., B. Pierrat, A. Xynos, K. Brecht, M. Simonen, A. Brungger, and J. Heim.** 2002. A microarray-based, integrated approach to identify novel regulators of cancer drug response and apoptosis. Oncogene **21:**8361–8371.
4. **Buettner, G. R., and B. A. Jurkiewicz.** 1993. Ascorbate free radical as a marker of oxidative stress: an EPR study. Free Radic. Biol. Med. **14:**49–55.
5. **Buffinton, G. D., and W. F. Doe.** 1995. Altered ascorbic acid status in the mucosa from inflammatory bowel disease patients. Free Radic. Res. **22:**131–143.
6. **Bunting, M., K. E. Bernstein, J. M. Greer, M. R. Capecchi, and K. R. Thomas.** 1999. Targeting genes for self-excision in the germ line. Genes Dev. **13:**1524–1528.
7. **Carrier, A., C. Nguyen, G. Victorero, S. Granjeaud, D. Rocha, K. Bernard, A. Miazek, P. Ferrier, M. Malissen, P. Naquet, B. Malissen, and B. R. Jordan.** 1999. Differential gene expression in CD3ε- and RAG1-deficient thymuses: definition of a set of genes potentially involved in thymocyte maturation. Immunogenetics **50:**255–270.
8. **Carrier, J., E. Aghdassi, J. Cullen, and J. P. Allard.** 2002. Iron supplementation increases disease activity and vitamin E ameliorates the effect in rats with dextran sulfate sodium-induced colitis. J. Nutr. **132:**3146–3150.
9. **Chamulitrat, W., and J. J. Spitzer.** 1997. Generation of nitro and superoxide radical anions from 2,4,6-trinitrobenzenesulfonic acid by rat gastrointestinal cells. Biochim. Biophys. Acta **1336:**73–82.
10. **Chan, A. T., E. L. Giovannucci, J. A. Meyerhardt, E. S. Schernhammer, G. C. Curhan, and C. S. Fuchs.** 2005. Long-term use of aspirin and nonsteroidal anti-inflammatory drugs and risk of colorectal cancer. JAMA **294:**914–923.
11. **Coussens, L. M., and Z. Werb.** 2002. Inflammation and cancer. Nature **420:**860–867.
12. **De Flora, S., A. Izzotti, F. D'Agostini, and R. M. Balansky.** 2001. Mechanisms of N-acetylcysteine in the prevention of DNA damage and cancer, with special reference to smoking-related end-points. Carcinogenesis **22:**999–1013.
13. **Duling, D. R.** 1994. Simulation of multiple isotropic spin-trap EPR spectra. J. Magn. Reson. B **104:**105–110.
14. **Dusetti, N. J., R. Tomasini, A. Azizi, M. Barthet, M. I. Vaccaro, F. Fiedler, J. C. Dagorn, and J. L. Iovanna.** 2000. Expression profiling in pancreas during the acute phase of pancreatitis using cDNA microarrays. Biochem. Biophys. Res. Commun. **277:**660–667.
15. **Finkel, T., and N. J. Holbrook.** 2000. Oxidants, oxidative stress and the biology of ageing. Nature **408:**239–247.
16. **Frejaville, C., H. Karoui, B. Tuccio, F. Le Moigne, M. Culcasi, S. Pietri, R. Lauricella, and P. Tordo.** 1995. 5-(Diethoxyphosphoryl)-5-methyl-1-pyrroline N-oxide: a new efficient phosphorylated nitrone for the in vitro and in vivo spin trapping of oxygen-centered radicals. J. Med. Chem. **38:**258–265.
17. **Greten, F. R., L. Eckmann, T. F. Greten, J. M. Park, Z. W. Li, L. J. Egan, M. F. Kagnoff, and M. Karin.** 2004. IKKbeta links inflammation and tumorigenesis in a mouse model of colitis-associated cancer. Cell **118:**285–296.
18. **Gupta, R. A., and R. N. Dubois.** 2001. Colorectal cancer prevention and treatment by inhibition of cyclooxygenase-2. Nat. Rev. Cancer **1:**11–21.
19. **Hershko, T., M. Chaussepied, M. Oren, and D. Ginsberg.** 2005. Novel link between E2F and p53: proapoptotic cofactors of p53 are transcriptionally upregulated by E2F. Cell Death Differ. **12:**377–383.
20. **Hussain, S. P., P. Amstad, K. Raja, S. Ambs, M. Nagashima, W. P. Bennett, P. G. Shields, A. J. Ham, J. A. Swenberg, A. J. Marrogi, and C. C. Harris.** 2000. Increased p53 mutation load in noncancerous colon tissue from ulcerative colitis: a cancer-prone chronic inflammatory disease. Cancer Res. **60:**3333–3337.
21. **Hussain, S. P., L. J. Hofseth, and C. C. Harris.** 2003. Radical causes of cancer. Nat. Rev. Cancer **3:**276–285.
22. **Itzkowitz, S. H., and X. Yio.** 2004. Inflammation and cancer IV. Colorectal cancer in inflammatory bowel disease: the role of inflammation. Am. J. Physiol. Gastrointest. Liver Physiol. **287:**G7–G17.
23. **Jiang, P. H., Y. Motoo, S. Garcia, J. L. Iovanna, M. J. Pebusque, and N. Sawabu.** 2006. Down-expression of tumor protein p53-induced nuclear protein 1 in human gastric cancer. World J. Gastroenterol. **12:**691–696.
24. **Jiang, P.-H., Y. Motoo, J. L. Iovanna, M.-J. Pebusque, M.-J. Xie, G. Okada, and N. Sawabu.** 2004. Tumor protein p53-induced nuclear protein 1 (*TP53INP1*) in spontaneous chronic pancreatitis in the WBN/Kob rat: drug effects on its expression in the pancreas. J. Pancreas **5:**205–216.

25. **Jiang, P. H., Y. Motoo, N. Sawabu, and T. Minamoto.** 2006. Effect of gemcitabine on the expression of apoptosis-related genes in human pancreatic cancer cells. World J. Gastroenterol. **12:**1597–1602.
26. **Karin, M.** 2006. Nuclear factor-kappaB in cancer development and progression. Nature **441:**431–436.
27. **Karp, S. M., and T. R. Koch.** 2006. Oxidative stress and antioxidants in inflammatory bowel disease. Dis. Mon. **52:**199–207.
28. **Kasparová, S., V. Brezova, M. Valko, J. Horecky, V. Mlynarik, T. Liptaj, O. Vancova, O. Ulicna, and D. Dobrota.** 2005. Study of the oxidative stress in a rat model of chronic brain hypoperfusion. Neurochem. Int. **46:**601–611.
29. **Khandoga, A., G. Enders, B. Luchting, S. Axmann, T. Minor, U. Nilsson, P. Biberthaler, and F. Krombach.** 2003. Impact of intraischemic temperature on oxidative stress during hepatic reperfusion. Free Radic. Biol. Med. **35:** 901–909.
30. **Kitajima, S., S. Takuma, and M. Morimoto.** 1999. Changes in colonic mucosal permeability in mouse colitis induced with dextran sulfate sodium. Exp. Anim. **48:**137–143.
31. **Klaunig, J. E., and L. M. Kamendulis.** 2004. The role of oxidative stress in carcinogenesis. Annu. Rev. Pharmacol. Toxicol. **44:**239–267.
32. **Krieglstein, C. F., W. H. Cerwinka, F. S. Laroux, J. W. Salter, J. M. Russell, G. Schuermann, M. B. Grisham, C. R. Ross, and D. N. Granger.** 2001. Regulation of murine intestinal inflammation by reactive metabolites of oxygen and nitrogen: divergent roles of superoxide and nitric oxide. J. Exp. Med. **194:**1207–1218.
33. **Kruidenier, L., and H. W. Verspaget.** 2002. Review article: oxidative stress as a pathogenic factor in inflammatory bowel disease—radicals or ridiculous? Aliment. Pharmacol. Ther. **16:**1997–2015.
34. **Marnett, L. J.** 2000. Oxyradicals and DNA damage. Carcinogenesis **21:**361–370.
35. **Martínez, N., M. Sanchez-Beato, A. Carnero, V. Moneo, J. C. Tercero, I. Fernandez, M. Navarrete, J. Jimeno, and M. A. Piris.** 2005. Transcriptional signature of Ecteinascidin 743 (Yondelis, Trabectedin) in human sarcoma cells explanted from chemo-naive patients. Mol. Cancer Ther. **4:**814–823.
36. **Munkholm, P.** 2003. Review article: the incidence and prevalence of colorectal cancer in inflammatory bowel disease. Aliment. Pharmacol. Ther. **2**(Suppl. 18)**:**1–5.
37. **Ogawa, K., M. Asamoto, S. Suzuki, K. Tsujimura, and T. Shirai.** 2005. Downregulation of apoptosis revealed by laser microdissection and cDNA microarray analysis of related genes in rat liver preneoplastic lesions. Med. Mol. Morphol. **38:**23–29.
38. **Ohkawa, H., N. Ohishi, and K. Yagi.** 1979. Assay for lipid peroxides in animal tissues by thiobarbituric acid reaction. Anal. Biochem. **95:**351–358.
39. **Okamura, S., H. Arakawa, T. Tanaka, H. Nakanishi, C. C. Ng, Y. Taya, M. Monden, and Y. Nakamura.** 2001. p53DINP1, a p53-inducible gene, regulates p53-dependent apoptosis. Mol. Cell **8:**85–94.
40. **Okayasu, I., S. Hatakeyama, M. Yamada, T. Ohkusa, Y. Inagaki, and R. Nakaya.** 1990. A novel method in the induction of reliable experimental acute and chronic ulcerative colitis in mice. Gastroenterology **98:**694–702.
41. **Okayasu, I., T. Ohkusa, K. Kajiura, J. Kanno, and S. Sakamoto.** 1996. Promotion of colorectal neoplasia in experimental murine ulcerative colitis. Gut **39:**87–92.
42. **Pietri, S., M. Culcasi, L. Stella, and P. J. Cozzone.** 1990. Ascorbyl free radical as a reliable indicator of free-radical-mediated myocardial ischemic and post-ischemic injury. A real-time continuous-flow ESR study. Eur. J. Biochem. **193:**845–854.
43. **Pietri, S., J. R. Seguin, P. d'Arbigny, K. Drieu, and M. Culcasi.** 1997. Ginkgo biloba extract (EGb 761) pretreatment limits free radical-induced oxidative stress in patients undergoing coronary bypass surgery. Cardiovasc. Drugs Ther. **11:**121–131.
44. **Pietri, S., J. R. Seguin, P. D. d'Arbigny, and M. Culcasi.** 1994. Ascorbyl free radical: a noninvasive marker of oxidative stress in human open-heart surgery. Free Radic. Biol. Med. **16:**523–528.
45. **Pravda, J.** 2005. Radical induction theory of ulcerative colitis. World J. Gastroenterol. **11:**2371–2384.
46. **Reddy, B. S.** 2004. Studies with the azoxymethane-rat preclinical model for assessing colon tumor development and chemoprevention. Environ. Mol. Mutagen. **44:**26–35.
47. **Rhodes, J. M., and B. J. Campbell.** 2002. Inflammation and colorectal cancer: IBD-associated and sporadic cancer compared. Trends Mol. Med. **8:**10–16.
48. **Rockenbauer, A., and L. Koretz.** 1996. Automatic computer simulation of ESR spectra. Appl. Magn. Reson. **10:**29–43.
49. **Salvemini, D., T. M. Doyle, and S. Cuzzocrea.** 2006. Superoxide, peroxynitrite and oxidative/nitrative stress in inflammation. Biochem. Soc. Trans. **34:**965–970.
50. **Sentjurc, M., S. Pecar, K. Chen, M. Wu, and H. Swartz.** 1991. Cellular metabolism of proxyl nitroxides and hydroxylamines. Biochim. Biophys. Acta **1073:**329–335.
51. **Seril, D. N., J. Liao, K. L. Ho, C. S. Yang, and G. Y. Yang.** 2002. Inhibition of chronic ulcerative colitis-associated colorectal adenocarcinoma development in a murine model by N-acetylcysteine. Carcinogenesis **23:**993–1001.
52. **Seril, D. N., J. Liao, G. Y. Yang, and C. S. Yang.** 2003. Oxidative stress and ulcerative colitis-associated carcinogenesis: studies in humans and animal models. Carcinogenesis **24:**353–362.
53. **Soriano, A., A. Salas, M. Sans, M. Gironella, M. Elena, D. C. Anderson, J. M. Pique, and J. Panes.** 2000. VCAM-1, but not ICAM-1 or MAdCAM-1, immunoblockade ameliorates DSS-induced colitis in mice. Lab. Investig. **80:**1541–1551.
54. **Suzuki, S., M. Asamoto, K. Tsujimura, and T. Shirai.** 2004. Specific differences in gene expression profile revealed by cDNA microarray analysis of glutathione S-transferase placental form (GST-P) immunohistochemically positive rat liver foci and surrounding tissue. Carcinogenesis **25:**439–443.
55. **Tachiiri, S., T. Katagiri, T. Tsunoda, N. Oya, M. Hiraoka, and Y. Nakamura.** 2006. Analysis of gene-expression profiles after gamma irradiation of normal human fibroblasts. Int. J. Radiat. Oncol. Biol. Phys. **64:**272–279.
56. **Tanaka, T., H. Kohno, R. Suzuki, Y. Yamada, S. Sugie, and H. Mori.** 2003. A novel inflammation-related mouse colon carcinogenesis model induced by azoxymethane and dextran sodium sulfate. Cancer Sci. **94:**965–973.
57. **Tardieu, D., J. P. Jaeg, J. Cadet, E. Embvani, D. E. Corpet, and C. Petit.** 1998. Dextran sulfate enhances the level of an oxidative DNA damage biomarker, 8-oxo-7,8-dihydro-2′-deoxyguanosine, in rat colonic mucosa. Cancer Lett. **134:**1–5.
58. **Tomasini, R., A. A. Samir, A. Carrier, D. Isnardon, B. Cecchinelli, S. Soddu, B. Malissen, J. C. Dagorn, J. L. Iovanna, and N. J. Dusetti.** 2003. TP53INP1s and homeodomain-interacting protein kinase-2 (HIPK2) are partners in regulating p53 activity. J. Biol. Chem. **278:**37722–37729.
59. **Tomasini, R., A. A. Samir, M. J. Pebusque, E. L. Calvo, S. Totaro, J. C. Dagorn, N. J. Dusetti, and J. L. Iovanna.** 2002. P53-dependent expression of the stress-induced protein (SIP). Eur. J. Cell Biol. **81:**294–301.
60. **Tomasini, R., A. A. Samir, M. I. Vaccaro, M. J. Pebusque, J. C. Dagorn, J. L. Iovanna, and N. J. Dusetti.** 2001. Molecular and functional characterization of the stress-induced protein (SIP) gene and its two transcripts generated by alternative splicing. SIP induced by stress and promotes cell death. J. Biol. Chem. **276:**44185–44192.
61. **Tomasini, R., M. Seux, J. Nowak, C. Bontemps, A. Carrier, J. C. Dagorn, M. J. Pebusque, J. L. Iovanna, and N. J. Dusetti.** 2005. TP53INP1 is a novel p73 target gene that induces cell cycle arrest and cell death by modulating p73 transcriptional activity. Oncogene **24:**8093–8104.
62. **Valko, M., H. Morris, M. Mazur, P. Rapta, and R. F. Bilton.** 2001. Oxygen free radical generating mechanisms in the colon: do the semiquinones of vitamin K play a role in the aetiology of colon cancer? Biochim. Biophys. Acta **1527:**161–166.
63. **Valko, M., C. J. Rhodes, J. Moncol, M. Izakovic, and M. Mazur.** 2006. Free radicals, metals and antioxidants in oxidative stress-induced cancer. Chem. Biol. Interact. **160:**1–40.
64. **Vanlandingham, J. W., N. M. Tassabehji, R. C. Somers, and C. W. Levenson.** 2005. Expression profiling of p53-target genes in copper-mediated neuronal apoptosis. Neuromol. Med. **7:**311–324.
65. **Vowinkel, T., M. Mori, C. F. Krieglstein, J. Russell, F. Saijo, S. Bharwani, R. H. Turnage, W. S. Davidson, P. Tso, D. N. Granger, and T. J. Kalogeris.** 2004. Apolipoprotein A-IV inhibits experimental colitis. J. Clin. Investig. **114:**260–269.
66. **Wiseman, H., and B. Halliwell.** 1996. Damage to DNA by reactive oxygen and nitrogen species: role in inflammatory disease and progression to cancer. Biochem. J. **313:**17–29.
67. **Wong, N. A., and D. J. Harrison.** 2001. Colorectal neoplasia in ulcerative colitis-recent advances. Histopathology **39:**221–234.
68. **Wurbel, M.-A., M. Malissen, D. Guy-Grand, E. Meffre, M. C. Nussenzweig, M. Richelme, A. Carrier, and B. Malissen.** 2001. Mice lacking the CCR9 CC-chemokine receptor show a mild impairment of early T- and B-cell development and a reduction in T-cell receptor $\gamma\delta^+$ gut intraepithelial lymphocytes. Blood **98:**2626–2632.
69. **Yoshida, K., H. Liu, and Y. Miki.** 2006. Protein kinase C delta regulates Ser46 phosphorylation of p53 tumor suppressor in the apoptotic response to DNA damage. J. Biol. Chem. **281:**5734–5740.
70. **Zhao, X., K. Demary, L. Wong, C. Vaziri, A. B. McKenzie, T. J. Eberlein, and R. A. Spanjaard.** 2001. Retinoic acid receptor-independent mechanism of apoptosis of melanoma cells by the retinoid CD437 (AHPN). Cell Death Differ. **8:**878–886.